ARTICLE NO. 79-4129

Experimental Study of Flow near the Trailing Edge of a Flat Plate in Rarefied Gas

L. Gottesdiener*
Laboratoire d'Aérothermique de l'Université Pierre et Marie Curie, Meudon, France

This experimental study of the trailing-edge region was made in a rarefied supersonic airflow in the following conditions: Mach = 2, $p_\infty = 60$ mHg, $Re_{L_\infty} = 1000$, $M_\infty/\sqrt{Re_{L_\infty}} = 0.06$. It is shown that in the region near the trailing edge, pressure, temperature, and density decrease, while velocity increases. The influence of the trailing edge is propagated upstream in the boundary layer to a distance $\delta/L \sim 1.2\, Re_{L_\infty}^{-3/8}$. The local skin friction coefficient decreases approaching the trailing edge. The contradiction between these results and recent theories exists because in our case, the no-slip condition at the wall is not satisfied. The velocity direction is determined from experimental values and the continuity equation: It is shown that the streamlines are inclined toward the plate when penetrating into the trailing-edge regions.

Nomenclature

a = thermal-accommodation coefficient
d = hot-wire diameter
h = convective heat-transfer coefficient
Kn = Knudsen number
L = length of the plate
M = Mach number
P = static pressure
Re_L = Reynolds number
T = temperature
T_{ad} = adiabatic-equilibrium temperature of the hot wire
U, U = velocity vector, velocity modulus
u, v = longitudinal and transversal velocity components
x, x = longitudinal axis coordinate
y, y = transversal axis coordinate
α = velocity angle with x
δ = length of upstream influence of the trailing edge
ϵ = $Re_{L_\infty}^{-1/8}$
ϵ_0 = emissivity coefficient of the hot wire
λ = molecular mean free path
χ = rarefaction parameter = $M_\infty/\sqrt{Re_{L_\infty}}$
ρ = density

Subscript

∞ = freestream conditions

Introduction

THE exact nature of flow in the trailing-edge region of flat plates seems now to be clearly known.[1] Recent computations made in a compressible flow by Daniels,[2] and in an incompressible flow by Jobe and Burggraf,[3] indicate that, at the trailing edge, the local skin friction increases to a finite value, whereas pressure decreases. The order of magnitude of the upstream influence is ϵ^3, where $\epsilon = Re_{L_\infty}^{-1/8}$. In the near wake, the flow is also quite well described: pressure exhibits a singularity at the end of the plate and increases from the trailing edge down.

However, to our knowledge, these theoretical studies have not received experimental confirmation. One may well ask why, since the boundary layer has been throughly investigated and, in the triple-deck theory,[1] for $\epsilon \ll 1$, the order of magnitude of the trailing-edge region ($L\epsilon^3$) is larger than that of the boundary-layer thickness ($L\epsilon^4$).

In an experimental investigation, the difficulty seems to originate from the fact that not only must the boundary-layer profiles be determined, but slight perturbations in these profiles must also be known. This requires far greater accuracy in experimental results, especially when the boundary-layer thickness is small. For these reasons, by selecting a rarefied airflow characterized by the parameters Mach = 2, $p_\infty = 60$ μmHg, $Re_{L_\infty} = 1000$, we obtained a very thick boundary layer on a 12-cm-long plate; this boundary layer is 2 cm thick at the end of the plate, thus enabling very fine scanning of the flow near the trailing edge. However, the no-slip condition at the wall is not satisfied, and this constitutes a major deviation from existing theoretical investigations. In fact, in our case, the rarefaction parameter $\chi = M_\infty/\sqrt{Re_{L_\infty}}$ is 0.06, placing the flow in slip conditions along the major part of the plate.[4]

Slip at the wall is a drawback in the problem at hand, because if a discontinuity in velocity exists at the trailing edge, the slip diminishes this discontinuity despite the existence of a high local-velocity gradient. In any case, the interpretation of the results must take account of the special experimental features introduced, particularly concerning slip at the wall, which distinguishes our work from other studies.

Experimental

Scanning was carried out with two instruments, the electron gun and the hot-wire probe, operating in rarefied gas. The former directly supplies density values by continuous profile recordings, first behind the upstream shock wave and then through the boundary layer until striking the plate, thus describing the entire flow.

The use of the hot-wire technique in rarefied gas raises major problems of implementation and processing of results. The problems consist of 1) an exact evaluation of radiation losses which are no longer negligible, as in nonrarefied-flow anemometry; and 2) the most complete possible elimination of heat losses from the hot wire by conduction in the supports, which play a nonnegligible role. These points were resolved by a considerable technical improvement, which consists of placing thermistors at the extremities of the hot wire, raised and kept at the same temperature at the wire by automatic regulation (Fig. 1). Moreover, thermocouples monitor the surface temperature where the hot wire is welded during all measurements and for each temperature.

Received May 17, 1978; revision received April 11, 1979.

Index categories: Rarefied Flows; Jets, Wakes, and Viscid-Inviscid Flow Interactions; Supersonic and Hypersonic Flow.

*Assistant Professor.

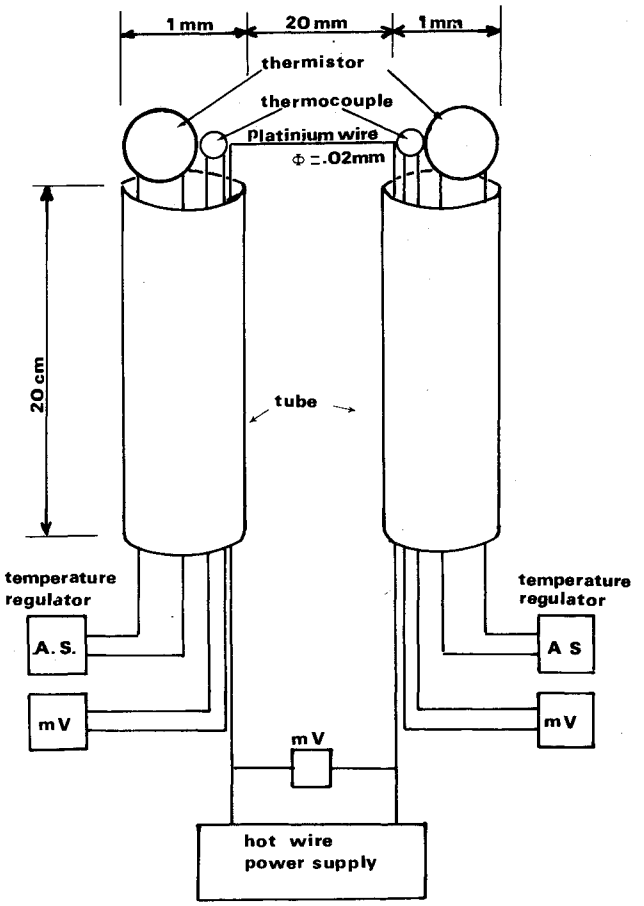

Fig. 1 Hot-wire anemometer.

Equipped with this system, the probe operates with extreme regularity. The hot wire itself consists of a platinum wire 20-mm long and 0.02-mm in diameter. The Knudsen number, $Kn=\lambda/d$, on the wire varies from 20 to 150 depending on the flow region, and is therefore always in free molecular regime. The emissivity ϵ_0 of the wire obtained by calibration varies slightly with operating temperature: $\epsilon_0=0.42$ at 80°C and $=0.45$ at 100°C. The accommodation coefficient a is 0.87, a value determined in the free jet.

The response of the hot wire makes it possible to determine the convection heat-transfer coefficient h and the adiabatic equilibrium temperature T_{ad} of the wire. The combination of h, T_{ad}, and density ρ by the use of the theory of free molecular flows makes it possible to raise the local velocity and the local Mach number. The pressure, temperature, and local skin-friction coefficient are then calculated, followed by the components u and v of velocity, using the continuity equation.

It should be noted that while gun recording supplies continuous density curves, this cannot be said of the hot-wire probe, for which a number of points are selected on a profile, fairly numerous and close together, in order for curve smoothing to improve accuracy.

Experimental Results

The special features of our flow are revealed by the curves representing variations in values (Figs. 2-7)—namely: a thick boundary layer and leading-edge shock wave; slight interaction between the boundary layer and the shock wave; significant slip at the wall; negative longitudinal pressure gradient; and specific flow region near the trailing edge.

The boundary-layer/shock-wave interaction is visible on the density profiles, which show that after a region of high gradients corresponding to penetration of the boundary layer, ρ continues to rise, although less sharply, up to the shock

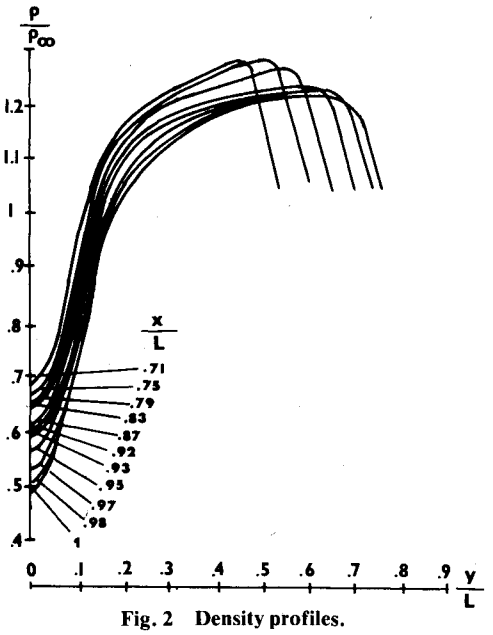

Fig. 2 Density profiles.

wave. Consequently, the intermediate flow is not uniform, which prevents accurate determination of the thickness of the boundary layer. It can nevertheless be evaluated at 2 cm, at least at the trailing edge, by limiting it to where a sudden change in curvature occurs. This result is in good agreement with rarefied boundary-layer results obtained in similar experimental conditions.[5] The velocity profiles exhibit a slip velocity (extrapolated to the wall) whose values are very important but in agreement with other experimental results.[6] The velocity and density decrease as temperature increases, implying that the gas is heated by friction and decelerated.

It is in the fluid streams adjacent to the wall that the trailing-edge region appears, as shown by the horizontal variations in ρ and U. Above a certain height ($y\simeq 7$ mm), the fluid streams propagate up to the trailing edge and beyond, in a uniform manner. Near the plate, however, the values vary abruptly at distances of about 10 mm from the trailing edge. This distance is reduced for the upper fluid streams, and the deformation no longer appears above 7 mm. Hence the trailing-edge region can be delimited upstream at a distance δ of 10 mm, giving the following equation as a function of Reynolds number:

$$\delta/L=10/120\simeq 1.2\,Re_{L_\infty}^{-1/3}$$

Our results also indicate how the values vary when penetrating the trailing-edge region. Density, temperature, and pressure decrease, whereas velocity increases. Hence, the influence consists of acceleration, cooling, and rarefaction of the fluid. Note that no discontinuity in the values exists at the trailing edge, but that the variations occur continuously in the near wake. A point exists in the near wake at which the density is a minimum, and this point gradually approaches the trailing edge.

On the upstream side, the influence of the trailing edge is sudden as soon as it is felt because it extends upstream, whereas on the downstream side the deformation develops gradually toward the wake.

To compare our study with the theoretical results obtained by the numerical resolution of Navier-Stokes equations, we have plotted our results and those of Daniel[2] in Fig. 8. In Ref. 2, the flow considered is quite different from ours because it is concerned with a compressible, nonrarefield gas, with no-slip conditions at the boundary layer. Irrespective of these experimental differences and the problems arising from the comparison of two flows, one of which is rarefied and the

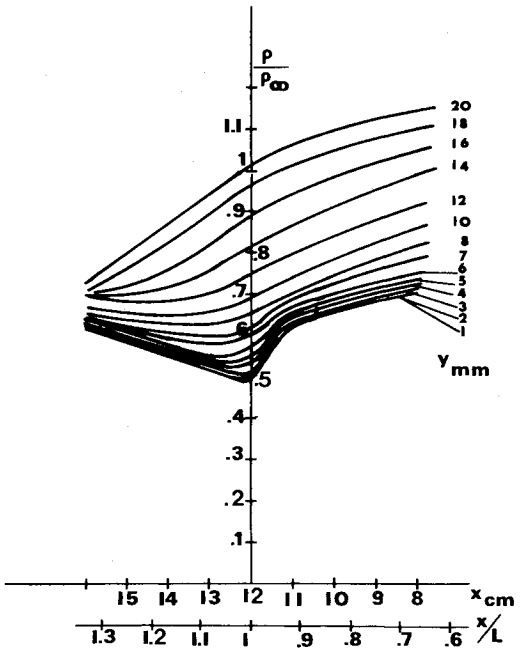

Fig. 3 Longitudinal density profiles.

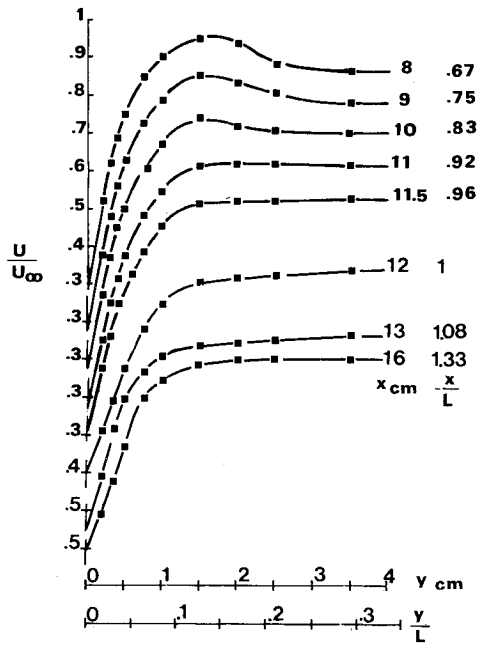

Fig. 4 Velocity profiles.

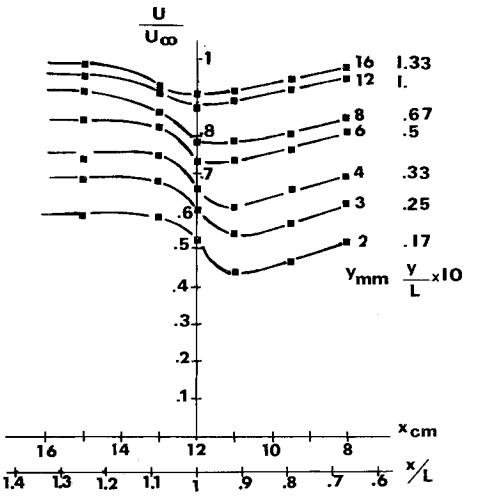

Fig. 5 Longitudinal velocity profiles.

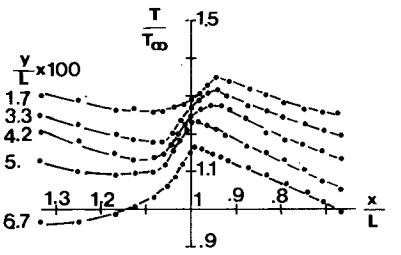

Fig. 6 Longitudinal temperature profiles.

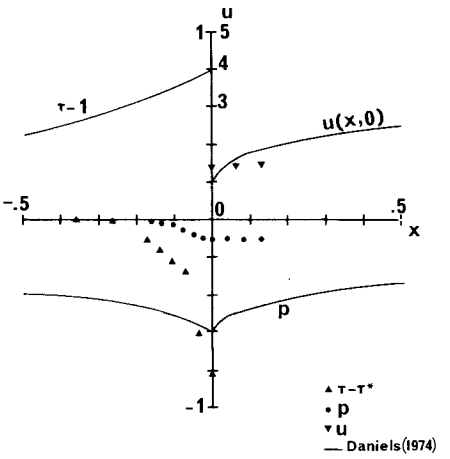

Fig. 7 Pressure, wall-velocity, and skin-friction evolutions.

other of which is not, the following observations may be made:

1) The value of our upstream distance of influence is smaller than the calculated value.

2) Our pressure gradient does not exhibit the discontinuity at the trailing edge anticipated by calculations.

3) Our local friction coefficient decreases approaching the trailing edge instead of increasing.

These discrepancies can be explained by the presence of slip at the wall: The acceleration effect of the trailing edge, which increases the velocity in the boundary-limit current tubes, acts simultaneously on the current tube directly adjacent to the plate, and the slip velocity therefore increases approaching the trailing edge, as shown in Figs. 4 and 5. Consequently, the transverse-velocity gradient decreases instead of increasing, as would be the case if the no-slip condition were satisfied at the wall. This result agrees with what is indicated by the slip-regime boundary-layer theory,[7] in which slip reduces friction while, elsewhere, the boundary layer exhibits a favorable longitudinal pressure gradient.

It may also be observed that the perturbation created by the trailing edge does not affect the boundary limit throughout its thickness, nor above, as indicated by the triple deck theory. This can also be explained by our rarefied-flow experimental conditions: First, the boundary layer is thicker and, second, slip at the wall partly attenuates the presence of the trailing edge and thus reduces its effect.

Finally, to describe the flow completely, we determined the direction of the velocity vector at every point from experimental readings. The calculation of the velocity components is presented in the appendix, where $U = ux + vy$ and $\alpha = (x, U)$. This procedure gives the value of α at every point, followed by the value of u and v. It may be noted that the angle α remains small throughout the boundary layer, so that

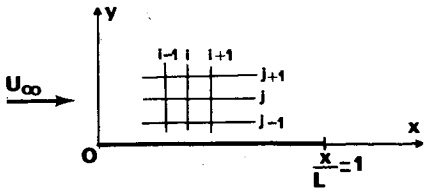

Fig. 8 Finite-difference grid.

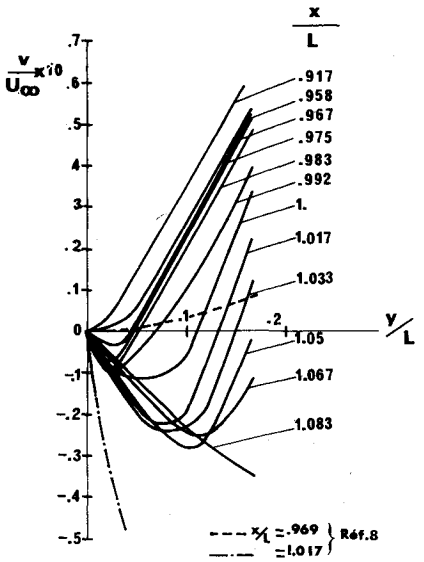

Fig. 9 Normal velocity-component profiles.

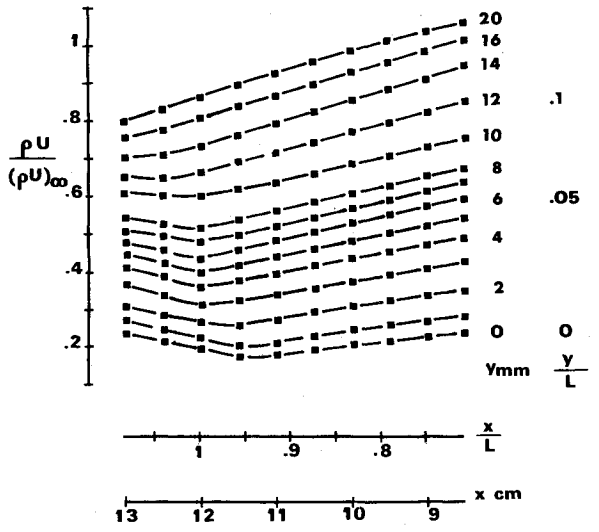

Fig. 10 Longitudinal evolution of $(\rho U)/(\rho U)_\infty$.

the streamlines are thus very close to the horizontal, deviating only slightly from the plate. At the entrance to the trailing-edge region α drops sharply, and is nullified and assumes negative values for points located very close to the trailing edge. Consequently, the streamlines which penetrate into the region of influence incline toward the trailing edge, and this effect is greater and occurs sooner as they approach the plate.

Hence, in the zone of influence, points are found for which the vertical component of velocity is negative (Fig. 10). Passing through the near wake, this component remains negative, but drops in amplitude. The comparison with values of v obtained theoretically by calculation indicates a satisfactory order of magnitude for v (Ref. 8) but singular behavior: Our value for the gradient of v along y is higher above the plate, while it is lower in the near wake, in comparison with the value indicated in Ref. 8.

Conclusions

The general agreement of our results with known results confirms the satisfactory operation of our equipment and the correctness of our scanning of the trailing-edge region. In our experimental conditions, the description of the flow leads to the following conclusions:

1) No discontinuity occurs at the trailing edge for any value, but this edge is surrounded by an original flow region included in the boundary layer, and which proceeds upstream to a distance δ such that $\delta/L \sim 1.2\, Re_{L\infty}^{-\frac{1}{2}}$. In this region, velocity increases, whereas pressure, density, and temperature decrease.

2) The local skin-friction coefficient declines to a nonzero value at the trailing edge, in accordance with the rarefied boundary-layer theory. This deviation from the theory derives from the fact that, as a basis for calculation, the latter imposes a no-slip condition at the wall along the entire plate up to the trailing edge, which does not apply in our case.

Appendix—Method for Calculating the Velocity Components

Taking the x axis parallel to the plate, the y axis normal, and the origin 0 at the leading edge, the mesh chosen is shown in Fig. 8.

The continuity equation is

$$(\rho u)_x + (\rho v)_y = 0 \tag{A1}$$

Equation (A1) can be written:

$$\frac{(\overline{\rho U})_x}{\overline{\rho U}} - \tan\alpha\alpha_x + \frac{(\overline{\rho U})_y}{\overline{\rho U}}\tan\alpha + \alpha_y = 0 \tag{A2}$$

where ρ is the density, U the velocity modulus, u and v the velocity components in the x and y directions, $\alpha = (\mathbf{0}\,\boldsymbol{x}, U)$, $u = U\cos\alpha$, $v = U\sin\alpha$, $\overline{\rho U} = \rho U/(\rho U)_\infty$, and $(\rho U)_\infty$ = freestream conditions. The $\overline{\rho U}$ profiles are shown in Fig. 10.

In Eq. (2), the quantities $(\overline{\rho U})_x/\overline{\rho U}$ and $(\overline{\rho U})_y/\overline{\rho U}$ are known experimentally in the entire flowfield. α_x and α_y are replaced by:

$$\alpha_x(i,j) = \frac{\alpha(i+1,j) - \alpha(i-1,j)}{[\Delta x]_{i-1}^{i+1}} \tag{A3}$$

$$\alpha_y(i,j) = \frac{\alpha(i,j+1) - \tfrac{1}{2}\{\alpha(i+1,j) + \alpha(i-1,j)\}}{[\Delta y]_j^{j+1}} \tag{A4}$$

For $y = 0$, we have $j = 1$, $\alpha = v = 0$, $u = U$, and Eq. (A2) gives

$$-\alpha_y(i,1) = \frac{(\overline{\rho U})x}{\overline{\rho U}}(i,1)$$

Equation (A4) written for $j = 1$ gives the values of $\alpha(i,2)$ which [using Eq. (3)] give the values of $\alpha_x(i,2)$. Integrating into Eq. (A2) we have $\alpha_y(i,2)$, making it possible to reach level $j = 3$ with Eq. (A4), and so on, for the whole boundary-layer thickness.

It is clear that the momentum equation could be applied as well as the continuity equation, but its application is far more complicated and cannot furnish the v values so directly. In fact, the use of the finite-difference scheme with the continuity equation gives the v values in a particularly simple and direct way.

It may be noted that the experimental uncertainties concerning ρ and U are present in the calculated values of v.

References

[1] Stewartson, K., *Advances in Applied Mechanics,* Vol. 14, 1974, pp. 146-234.
[2] Daniels, P.G., *Quarterly Journal of Applied Mathematics,* Vol. 27, 1974, pp. 175-190.
[3] Jobe, C.E. and Burggraf, O.A., *Proceedings of the Royal Society,* Series A, Vol. 340, 1974, pp. 91-111.
[4] "Mechanics of Rarefied Gases," Navord Report 1488, Vol. 5, Section 16.
[5] Rogers, E.W.E. and Berry, C.J., "Rarefied Gas Dynamics," *4th International Symposium on Rarefied Gas Dynamics,* Vol. 1, Toronto, Academic Press, New York, 1964, p. 584.
[6] Becker, M., "Rarefied Gas Dynamics," *6th International Symposium on Rarefied Gas Dynamics,* Vol. 1, Academic Press, New York, 1969, pp. 515-526.
[7] Kogan, M.N., *Rarefied Gas Dynamics,* Plenum Press, New York, 1969, p. 395.
[8] Plotkin, A. and Flugge-Lotz, I., *Journal of Applied Mechanics,* Vol. 12, 1968, pp. 625-630.